Gyroscopic and Damping Effects on the Stability of a Noncontacting Flexibly-Mounted Rotor Mechanical Face Seal

ITZHAK GREEN
The George W. Woodruff School of Mechanical Engineering
Georgia Institute of Technology
Atlanta, Georgia 30332-0405, USA

INTRODUCTION

A noncontacting flexibly-mounted rotor mechanical face seal is shown in Fig. 1. The flexibly-mounted rotor is supported by circumferential springs and by a secondary seal (usually an elastomeric O-ring), and the rotor is driven by two positive drive devices which engage it mechanically to the rotating shaft. Because of manufacturing and assembly imperfections the stator and the rotor are misaligned with respect to the axis of shaft rotation. The ability of the flexibly-mounted rotor to respond to the stator misalignment with minimum relative misalignment between the rotor and the stator (to prevent failure due to face contact and to minimize fluid leakage) is of prime importance, provided that the system stability requirements have also been fulfilled.

Several mechanisms can induce instabilities. For example: (1) Fluid boiling and phase change can yield a total film collapse (Hughes and Chao, 1980) or a limit cycle oscillation (Basu and Hughes, 1987). (2) Temperature and pressure fields induce thermoelastic distortions (causing face rotation) which has been found to have a major effect during start-up and other transient operation (Doust and Parmer, 1987). (3) Dynamic instability, (which is the subject of this work), can emerge from hydrostatic and hydrodynamic effects as well as from system properties, e.g., inertia and flexible support stiffness and damping.

The case where the stator is flexibly mounted and the rotor is rigidly attached to a rotating shaft has been the subject of extensive theoretical and experimental dynamic investigations during the last two decades (Etsion, 1982 and 1985). A comprehensive analytical solution has recently been presented using perturbation techniques (Green and Etsion, 1985), as well as a numerical solution which accounts for all nonlinearities, i.e., cavitation, curvature, and finite disturbances (Green and Etsion, 1986a). In contrast, the case of current interest where the rotor is flexibly-mounted while the stator is fixed has only been generally described (Nau, 1981) and treated (Metcalfe, 1981).

This paper will construct the equations of motion in the axial and angular modes as affected by the generalized applied forces (flexible support and fluid film effects) and the generalized dynamic forces. The dynamic characteristics of elastomeric O-rings in the axial-twist-shear mode has been studied experimentally (Green and Etsion, 1986b) yielding empirical expressions for stiffness and damping coefficients. The rotordynamic (fluid-film) coefficients for the present investigation are also readily available (Green, 1987). The above constitute the generalized applied forces. The generalized dynamic forces for the flexibly-mounted configuration have been introduced by associating the kinematic constraint imposed by the positive drive devices with the coupling effect in a universal joint (Green and Etsion, 1986c). We will investigate here the equations of motion and provide stability criteria as prerequisite conditions for safe operation at steady state.

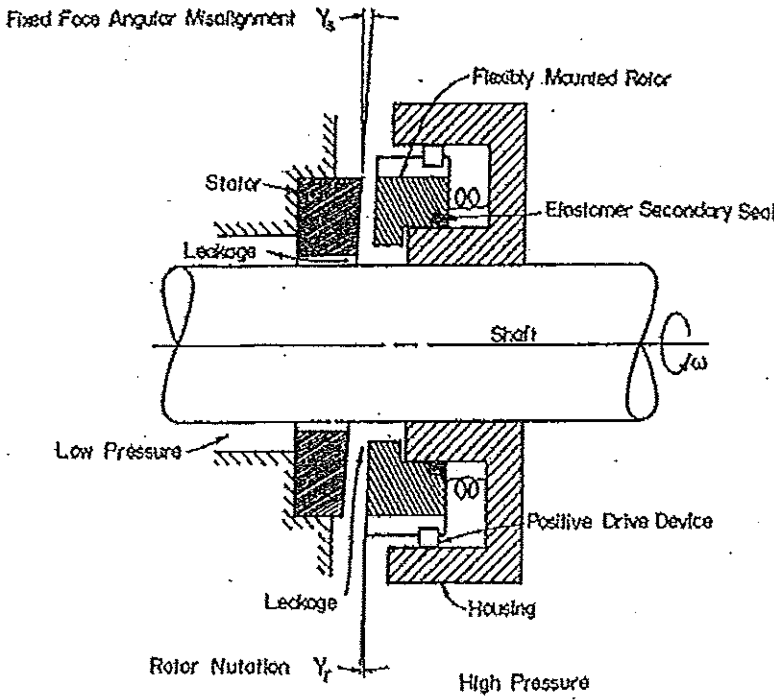

Figure 1. Schematic of a Flexibly Mounted Rotor Face Seal.

THE KINEMATIC MODEL AND THE DYNAMIC FORCES

The mechanical system of Fig. 1 can be generally represented by the model of Fig. 2. The shaft rotates at a constant angular velocity, ω, about axis Z of a rotating reference XYZ, where axis X passes through one of the positive drive devices (see Fig. 1). Axis ξ is an arbitrary inertial axis, such that the angle assumed between ξ and X equals to ωt. The two remaining inertial axes, η and ζ (of the inertial reference $\xi\eta\zeta$) are shown in Fig. 1, where axis ζ coincides with the axis of shaft rotation, Z. The flexibly-mounted rotor can move axially along Z and can also tilt about axis x by an amount γ_r (the nutation angle) measured between the axis of shaft rotation, Z, and the normal to the rotor surface, i.e., the polar axis z. Reference xyz is also rotating, so that axis x is always in the XY plane (i.e., x is orthogonal to Z at all times) and it is shifted by the relative precession angle, ψ, from the driving axis, X, or by the absolute precession angle, ψ_r, measured from the inertial axis, ξ, such that

$$\psi_r = \omega t + \psi \tag{1}$$

(All parameters are dimensional until further notice).

The third Euler angle, ϕ, is the relative spin which takes place about axis z. However, the three Euler angles γ_r, ψ_r, and ϕ are not independent due to the constraint imposed by the two positive drive devices which force the rotor to return to its original position relative to the housing after completing one cycle. The kinematical relationship between the three angles has been thoroughly studied by Green and Etsion (1986c). For small nutation (tilt) angles the spin can be approximated by $\dot{\phi} = -\dot{\psi}$, or with the aid of eq. (1) $\dot{\phi} = \omega - \dot{\psi}_r$ and the components of the dynamic moment have the form

$$T_x = I\left(\ddot{\gamma}_r - \dot{\psi}_r^2\,\gamma_r\right) + I_z\omega\,\dot{\psi}_r\gamma_r \tag{2-a}$$

$$T_y = I\left(\ddot{\psi}_r\gamma_r + 2\dot{\psi}_r\dot{\gamma}_r\right) - I_z\omega\,\dot{\gamma}_r \tag{2-b}$$

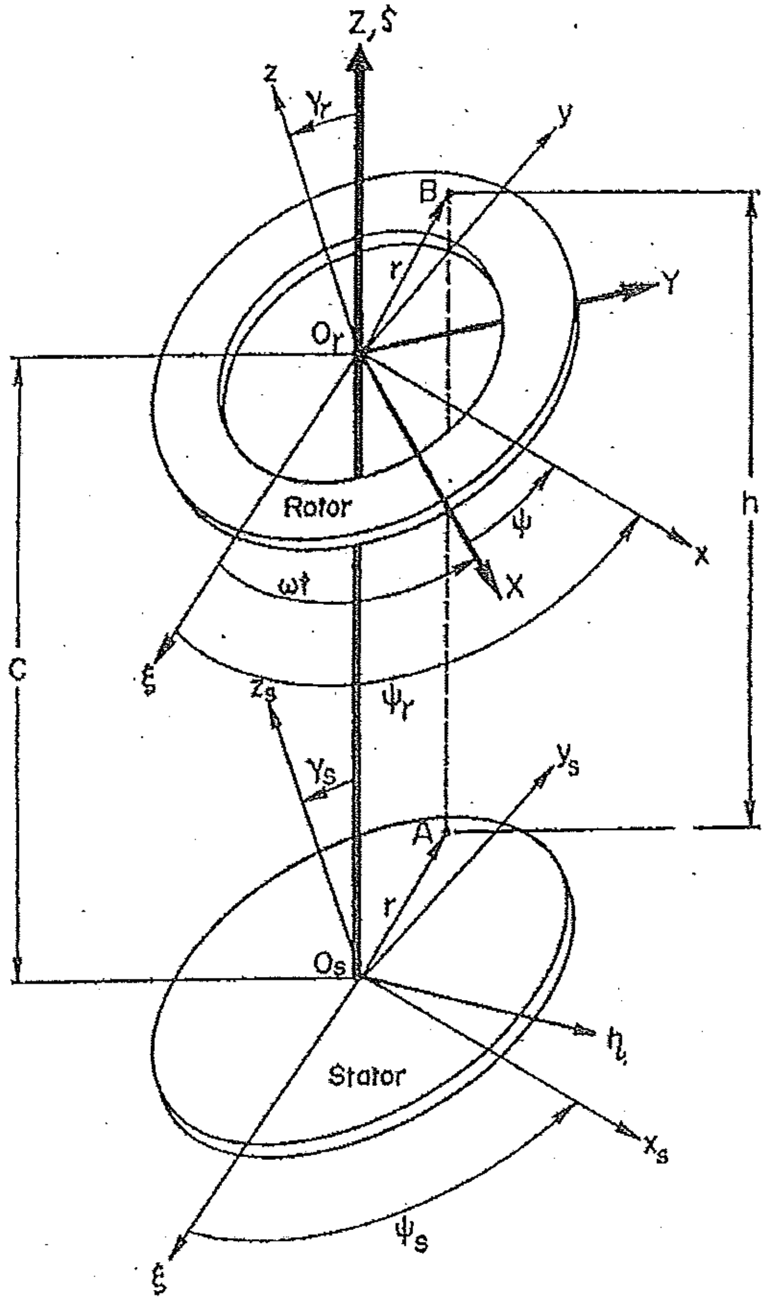

Figure 2. Seal Model and Coordinate System.

where I and I_z are the rotor transverse and polar moments of inertia. The last component, T_2, is of order γ_r^2 and is therefore neglected.

It will be useful to have the components of the dynamic moment expressed also in an inertial reference. This can be accomplished by using the following transformation

$$\{L\}_{\xi\eta\zeta} = [T]\ \{L\}_{xyz}$$

where $\{L\}_{\xi\eta\varsigma}$ and $\{L\}_{xyz}$ are the angular momenta corresponding to the inertial system $\xi\eta\varsigma$ and the rotating system xyz, respectively. The transformation matrix $[\gamma]$ can be found in Meriam (1971, pp. 304-305). Explicitly we have

$$\begin{Bmatrix} L_\xi \\ L_\eta \\ L_\varsigma \end{Bmatrix} = \begin{bmatrix} \cos\psi_r & -\cos\gamma_r\sin\psi_r & \sin\gamma_r\sin\psi_r \\ \sin\psi_r & \cos\gamma_r\cos\psi_r & -\sin\gamma_r\cos\psi_r \\ 0 & \sin\gamma_r & \cos\gamma_r \end{bmatrix} \begin{Bmatrix} I\dot{\gamma}_r \\ I\dot{\psi}_r\sin\gamma_r \\ I_z\omega \end{Bmatrix} \tag{3}$$

where $\{L\}_{xyz}$ has been taken from Green and Etsion (1986c).

By defining γ_ξ and γ_η as rotor cartesian tilts which relate to the angles γ_r and ψ_r by

$$\gamma_\xi = \gamma_r\cos\psi_r \tag{4-a}$$

$$\gamma_\eta = \gamma_r\sin\psi_r \tag{4-b}$$

and using the approximations $\sin\gamma_r \simeq \gamma_r$, and $\cos\gamma_r \simeq 1$, the angular momentum of eq. (3) has the final form

$$L_\xi = I\dot{\gamma}_\xi + I_z\omega\gamma_\eta \tag{5-a}$$

$$L_\eta = I\dot{\gamma}_\eta - I_z\omega\gamma_\xi \tag{5-b}$$

$$L_\varsigma = I_z\omega \tag{5-c}$$

The time derivative of the angular momentum provides us with the following cartesian components of the dynamic moment

$$T_\xi = I\ddot{\gamma}_\xi + I_z\omega\dot{\gamma}_\eta \tag{6-a}$$

$$T_\eta = I\ddot{\gamma}_\eta - I_z\omega\dot{\gamma}_\xi \tag{6-b}$$

$$T_\varsigma = 0 \tag{6-c}$$

containing the gyroscopic terms $I_z\omega\dot{\gamma}_\eta$ and $-I_z\omega\dot{\gamma}_\xi$.

In practical applications, due to manufacturing and assembly imperfections, the rotor and the stator may be skewed with respect to the axis of shaft rotation. The initial rotor misalignment, γ_{ri}, is caused by an imperfect elastic foundation. Without losing generality γ_{ri} is assumed to take place about the driving axis X. To obtain the contribution of this misalignment to the system of applied forces, we may look at the problem by presuming instead that the rotor is perfectly aligned initially but that some moment M_{Xi} causes it to tilt by the amount γ_{ri} about the X axis. Thus, if we designate the support angular stiffness by K_{s11} (which includes spring and secondary seal stiffnesses), then

$$M_{Xi} = K_{s11} \gamma_{ri} \tag{7}$$

This moment is a rotating vector of constant magnitude.

Flexural stiffness and damping coefficients of the spring and the secondary seal are either known or can be physically determined (see for example Green and Etsion (1986b)). The angular coefficients (designated by the subscript 11) have been derived from the axial ones (designated by the subscript 33) by Green and Etsion (1985) to be

$$K_{s11} = \frac{1}{2} K_{s33} r_s^2 \tag{8-a}$$

$$D_{s11} = \frac{1}{2} D_{s33} r_s^2 \tag{8-b}$$

$$K_{s12} = D_{s11} \dot{\psi} \tag{8-c}$$

where subscript s represents support coefficients and r_s is a general radial location of that flexible support. (Note that if the spring and the secondary seal have two different radial locations, then K_{s11} has to be calculated for each element separately, and then combine K_{s33} and K_{s11} together as springs in parallel).

The stator misalignment, γ_s, on the other hand, takes place about a stationary axis x_s where ψ_s is an arbitrary angle measured between x_s and ξ. The angle γ_s is measured between the axis of shaft rotation, Z, and the normal to the stator surface, z_s (see Fig. 2). This misalignment contributes to the system of applied forces via the fluid film.

The clearance, C, between the rotor and the stator is very small; thus γ_r and γ_s must also be very small and can be treated as vectors. Hence, the relative misalignment of the rotor with respect to the stator, γ, is given by the following vector subtraction:

$$\vec{\gamma} = \vec{\gamma}_r - \vec{\gamma}_s \tag{9}$$

The relative position is described by a new reference 123 as shown in Fig. 3. This system is free to rotate within the rotor plane so that axis 1 (about which the rotor relative tilt, γ, takes place) is always parallel to the stator plane and axis 2 is always directed toward the point of maximum distance between the disks. The relative shift angle, ϕ_1, is measured between axes X and 1.

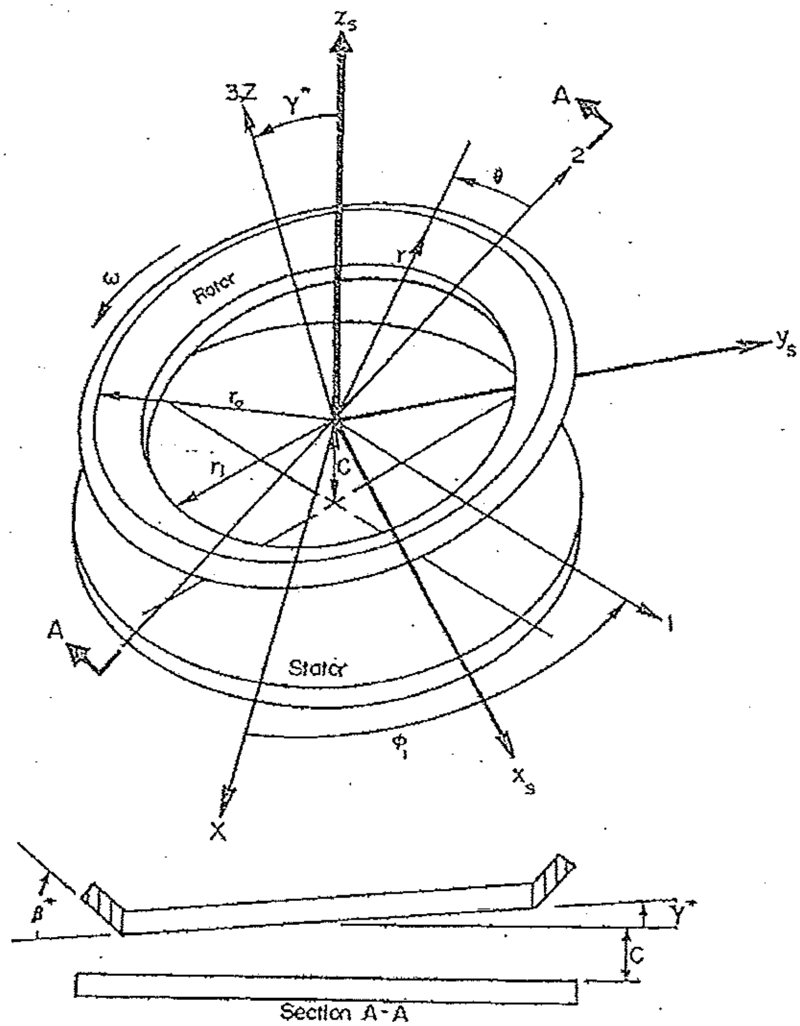

Figure 3. Relative Position Between Rotor and Stator.

As shown in section A-A the rotor surface may have a coning angle, β. The coning, combined with a radial pressure gradient across the faces, generates axial and angular stiffness coefficients. These coefficients along with the corresponding damping coefficients have been derived, and the influence of both the coning angle and the direction of the pressure drop have been fully discussed (Green, 1987). That study provides the linearized rotor dynamic coefficients in the form of stiffness and damping, K_{fij} and D_{fij}, respectively (where subscript f designates fluid film coefficients). The zeroth order (but non-zero) terms, K_{f11}, K_{f12}, K_{f33}, D_{f11}, and D_{f33} are summarized in Table 1. All other terms equal zero identically or are of a higher order (Green and Etsion, 1983). The stiffness coefficients K_{f11} and K_{f33} are directly proportional to the pressure drop and to the coning angle (hydrostatic effect), while the cross coupled coefficient K_{f12} is an outcome of the hydrodynamic and squeeze effects and possesses a value $K_{f12} = D_{f11} (\phi_1 + \omega/2)$.

		$j = 1$	$j = 2$	$j = 3$
$i = 1$	K	$\pi(P_a - P_s)(\beta R_s - 1)E_s^2$	$2\pi R_m^3 G_s\left(\dot{\phi}_1 + \frac{1}{2}\right)$	0
	D	$2\pi R_m^3 G_s$	0	
$i = 2$	K & D	0	0	0
$i = 3$	K	0	0	$\pi(P_a - P_s)\frac{2\beta}{R_m}E_s^2$
	D			$4\pi R_m G_s$

$$E_s = \frac{(1-R_s)R_m}{2+\beta(1-R_s)}$$

$$G_s = \frac{\ln[1+\beta(1-R_s)] - 2\frac{\beta(1-R_s)}{2+\beta(1-R_s)}}{\beta^3(1-R_s)^2}$$

$$G_{x,y,z} = \frac{1-R_s}{12}$$

In general K_{ij} (or D_{ij}) are defined as restoring (or dissipating) applied forces along j due to a unit displacement (or a unit time derivative of the displacement) at i. Hence, the applied generalized forces of the flexible support are given in the rotating system xyz by

$$F_{sZ} = - K_{s33}Z - D_{s33}\dot{Z} \tag{10-a}$$

$$M_{sx} = - K_{s11}\gamma_r - D_{s11}\dot{\gamma}_r \tag{10-b}$$

$$M_{sy} = - K_{s12}\gamma_r \tag{10-c}$$

and those of the fluid film are given in the relative system 123 by

$$F_{fZ} = - K_{f33}Z - D_{f33}\dot{Z} \tag{11-a}$$

$$M_{f1} = - K_{f11}\gamma - D_{f11}\dot{\gamma} \tag{11-b}$$

$$M_{f2} = - K_{f12}\gamma \tag{11-c}$$

Tilts and moments are best described in the vector diagram of Fig. 4. This diagram shows the various reference systems and their relative positions with respect to each other. Because of small tilt angles (which enables a vectorial treatment) we may neglect the deviation of planes xy (see Fig. 2) and 12 (see Fig. 3) from plane XY, where the normals to these planes, z, 3, and Z, respectively, are at all times contained within a cone of a very small vertex angle. Hence, with simple projections of the various moment components the equations of motion can be constructed in either the rotating reference or the inertial reference.

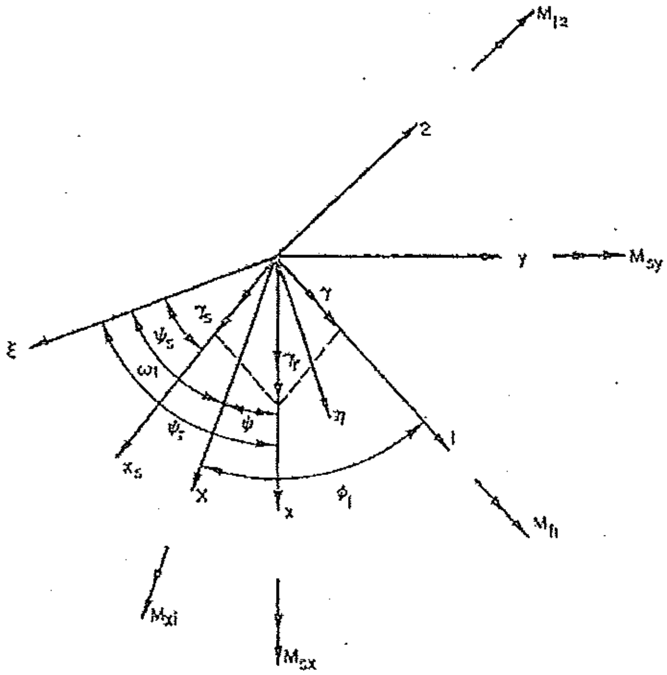

FIG. 4 VECTOR DIAGRAM OF MOMENTS AND TILTS

THE EQUATIONS OF MOTION

In the following discussion dimensional parameters will be identified by an asterisk to distinguish them from their corresponding dimensionless values. (For conciseness, the normalization is not performed here in detail. However, the dimensional and the corresponding dimensionless variables are summerized in the nomenclature). Also, the subscript 11 will be omitted from the angular stiffness and damping coefficients K, and D, respectively. Only subscript 33 will be retained for axial coefficients K_{33} and D_{33}.

The equations of motion are obtained by equating the dynamic forces and the applied forces. The equation of motion in the axial degree of freedom, Z, is rather simple:

$$m\ddot{Z} = F_Z$$

where m is the rotor mass and F_Z is the sum of the forces given in eqs. (10-a) and (11-a). Hence,

$$m\ddot{Z} + D_{33}\dot{Z} + K_{33}Z = 0 \qquad (12)$$

where

$$K_{33} = K_{s33} + K_{f33} \quad ; \quad D_{33} = D_{s33} + D_{f33}$$

The details of the derivation of the equations of motion in the angular mode are given in Appendix A. Eqs. (A-16) provide the governing equations in the inertial system $\xi\eta\varsigma$:

$$I\ddot{\gamma}_\xi + I_z\dot{\gamma}_\eta + D\dot{\gamma}_\xi + B\gamma_\eta + K\gamma_\xi = \gamma_s\left[K_f\cos\psi_s + \frac{1}{2}D_f\sin\psi_s\right] + K_s\gamma_{ri}\cos\omega t \tag{13-a}$$

$$I\ddot{\gamma}_\eta - I_z\dot{\gamma}_\xi + D\dot{\gamma}_\eta - B\gamma_\xi + K\gamma_\eta = \gamma_s\left[K_f\sin\psi_s - \frac{1}{2}D_f\cos\psi_s\right] + K_s\gamma_{ri}\sin\omega t \tag{13-b}$$

These prove to be linear equations, coupled in the two cartesian tilts γ_ξ and γ_η. It is clearly seen that γ_s and γ_{ri} have the nature of forcing functions. Hence, the overall solution could be pursued by solving for each forcing function separately and combining the responses at the end (superposition). Based on physical reasoning, however, it would be more useful to solve the equations in the rotating system, as this system is more natural to the problem. The equations of motion expressed in the rotating system are given in Eqs. (A-17), which read

$$I\left[\ddot{\gamma}_r - \dot{\psi}_r^{\,2}\gamma_r\right] + I_z\dot{\psi}_r\gamma_r = -K\gamma_r - D\dot{\gamma}_r + K_s\gamma_{ri}\cos\psi + \gamma_s\left[K_f\cos\rho' - \frac{1}{2}D_f\sin\rho'\right] \tag{14-a}$$

$$I\left[\ddot{\psi}_r\gamma_r + 2\dot{\psi}_r\dot{\gamma}_r\right] - I_z\dot{\gamma}_r = -D\dot{\psi}\gamma_r - \frac{1}{2}D_f\gamma_r - K_s\gamma_{ri}\sin\psi - \gamma_s\left[K_f\sin\rho' + \frac{1}{2}D_f\cos\rho'\right] \tag{14-b}$$

STABILITY THRESHOLD

Axial Mode:

The equation of motion in the axial mode, eq. (12), is totally identical to the equation of motion given by Green and Etsion (1985) for a flexibly-mounted stator seal (see eq. (11) there). As this is a small perturbation analysis where the equations of motion in the axial and angular mode are decoupled, it really does not matter which element is flexibly mounted. Therefore, the conditions for stability in the axial mode are just repeated from the earlier study. Specifically, all the coefficients in eq. (12) must be positive, and since m and D_{33} are always positive, the only remaining requirement is $K_{33} > 0$, or $K_{s33} + K_{f33} > 0$. Again, K_{s33} is always positive, but in practical applications K_{s33} is also several orders of magnitude smaller than K_{f33}. Hence, the condition $K_{f33} > 0$ is pratically necessary to guarantee hydrostatic stability. Using Table 1, this condition translates into

$$(P_o - P_i)\,\beta > 0 \tag{15}$$

This condition indicates that, in order to assure stability, the pressure induced flow must prevail in a converging gap. While $\beta = 0$ (corresponding to a flat face seal) satisfies the condition for stability, the value $\beta_{opt} = 2/(1 - R_i)$ establishes a maximum restoring axial stiffness for an inward flow seal, as proven by Green and Etsion (1983). In the case of an outward flow seal, the axial fluid film stiffness increases monotonically with the negative coning or dishing angle, β, to a maximum set by geometrical constraints (Green, 1987).

Angular Mode:

As demonstrated in eqs. (13), γ_s and γ_{ri} are forcing functions. Stability, however, is determined from the investigation of the homogeneous part of the equations yielding the transient response solution. Hence, by setting γ_s and γ_{ri} to zero, eqs. (13) become

$$I\ddot{\gamma}_\xi + I_z\dot{\gamma}_\eta + D\dot{\gamma}_\xi + B\gamma_\eta + K\gamma_\xi = 0 \tag{16-a}$$

$$I\ddot{\gamma}_\eta - I_z\dot{\gamma}_\xi + D\dot{\gamma}_\eta - B\gamma_\xi + K\gamma_\eta = 0 \tag{16-b}$$

It is useful to use complex notation, noting that the rotor nutation, γ_r, is a vector sum of the two tilts γ_ξ and γ_η such that $\gamma_r = \gamma_\xi + i\,\gamma_\eta$ where $i = \sqrt{-1}$, and ξ and η represent, respectively, the real and imaginary axes of the complex plane. Multiplying eq. (16-b) by i and adding it to eq. (16-a) results in

$$I\ddot{\gamma}_r + D\dot{\gamma}_r + K\gamma_r - i\left(I_z\dot{\gamma}_r + B\gamma_r\right) = 0 \tag{17}$$

For this linear system, the following solution is assumed: $\gamma_r = \gamma_{ro}\, e^{\lambda t}$. Substituting this solution into eq. (17) yields

$$I\lambda^2 + D\lambda + K - i\left(I_z\lambda + B\right) = 0$$

Multiplying the above equation by its complex conjugate yields the characteristic equation

$$a_4\lambda^4 + a_3\lambda^3 + a_2\lambda^2 + a_1\lambda + a_0 = 0 \tag{18}$$

where $a_0 = K^2 + B^2$ $\qquad a_1 = 2DK + 2I_zB$ $\qquad a_2 = 2IK + D^2 + I_z^2$

$a_3 = 2ID$ $\qquad a_4 = I^2$

The necessary condition for stability requires that all the coefficients a_i in eq. (18) be positive. Since the moments of inertia I and I_z are positive, and the damping D_s and D_f are also positive, (so that D > 0 and B > 0) the coefficients a_0, a_3, and a_4 are unconditionally positive. In order to also satisfy $a_1 > 0$ and $a_2 > 0$, we see that some negative values of K are allowed (depending of course on the values of I, I_z, D, and B). It is reasonable, however, to require that the overall angular stiffness, $K = K_f + K_s$, be also positive, since K_f (which is much larger than K_s in practical applications) depends directly on the pressure drop, $P_o - P_i$, which can be substantial. Hence, using Table 1 for K_f results in a conservative, but quite realistic condition

$$\left(P_o - P_i\right)\left(\beta R_i - 1\right) > 0 \tag{19}$$

This condition has been thoroughly discussed, and the two cases of inward and outward flows have been compared (Green, 1987). It is seen from eq. (19) that for inward flow ($P_o - P_i > 0$) the coning angle β should be greater than a critical coning $\beta_{cr} = 1/R_i$. An optimal coning, $\beta_{opt} = 2/R_i(1 - R_i)$ (Green and Etsion, 1983), not just fulfills this requirement but also produces maximum restoring angular stiffness. However, as found in the study on the rotor dynamic coefficient (Green, 1987), the case of outward flow ($P_o - P_i < 0$ and $\beta < 0$) outperforms unconditionally the case of inward flow. Also, when eq. (19) is fulfilled outward flow always produces positive stiffness. From this pure dynamic investigation outward flow is preferable.

Once the necessary conditions, $a_i > 0$ for $i = 0,...,4$, are fulfilled the Routh-Hurwitz stability criteria for eq. (18) degenerate into (Arnold and Maunder, 1961, pp. 453-454)

$$a_1 a_2 a_3 - a_0 a_3^2 - a_1^2 a_4 > 0 \tag{20}$$

which is an additional requirement to guarantee stability. Substituting the values of the coefficients a_i in eq. (20), yields after simplification the last condition for stability

$$KD^2 + I_z BD - IB^2 > 0 \tag{21}$$

Obviously, stability threshold occurs when

$$KD^2 + I_z BD - IB^2 = 0 \tag{22}$$

It is now of interest to understand the physical phenomenon which leads to eq. (22). By definition the stability analysis is performed for the case where the forcing functions are absent. In other words, we investigate the homogeneous part of the equations of motion as if the stator and the rotor were perfectly aligned with respect to the axis of shaft rotation. For this case, when γ_s and γ_{ri} are set to zero, the rotating references 123 and xyz coincide (see eq. (9)), and the equations of motion (14) in the rotating reference take the form

$$I\left[\ddot{\gamma}_r - \dot{\psi}_r^2 \gamma_r\right] + I_z \dot{\psi}_r \gamma_r = -K\gamma_r - D\dot{\gamma}_r \tag{23-a}$$

$$I\left[\ddot{\psi}_r \gamma_r + 2\dot{\psi}_r \dot{\gamma}_r\right] - I_z \dot{\gamma}_r = -D_f\left(\dot{\psi} + \frac{1}{2}\right)\gamma_r - D_s \dot{\psi} \gamma_r \tag{23-b}$$

where D in eq. (14-b) has been replaced by its definition (A16-d).

Any disturbance introduced in a stable system will eventually die out, and the rotor will return to its natural position of being aligned with respect to the shaft axis of rotation. On the other hand, in an unstable system any disturbance will grow exponentially with time, causing seal failure in the form of touchdown or excessive leakage. At stability threshold the system is indifferent to disturbances and any arbitrary disturbance will remain in the system indefinitely. Hence, at stability threshold the flexibly-mounted rotor possesses an arbitrary constant nutation angle and precesses at a constant rate. Such a motion is known as "steady state precession" or "uniform precession." This situation is represented by the following conditions:

$$\gamma_r = \text{const} \quad , \quad \dot{\psi}_r = \text{const} \quad ; \qquad \ddot{\psi}_r = \ddot{\gamma}_r = \dot{\gamma}_r = 0$$

The equations of motion (23) then become

$$- I\dot{\psi}_r^2\gamma_r + I_z\dot{\psi}_r\gamma_r = - K\gamma_r \tag{24-a}$$

$$0 = - D_f\left(\dot{\psi} + \frac{1}{2}\right)\gamma_r - D_s\dot{\psi}\,\gamma_r \tag{24-b}$$

From eq. (24-b) the relative precession rate at stability threshold has the value

$$\dot{\psi}_{ST} = - \frac{D_f}{2(D_f + D_s)} \tag{25}$$

The minus sign in eq. (25) indicates that the rotor precesses within the rotating housing in a direction opposite to the shaft rotation. This behavior is called "retrograde precession" or "backward whirl." When the support damping is absent (or is negligible compared to fluid damping) the relative precession rate equals half of the shaft speed, and may be called the "retrograde half frequency whirl."

The absolute precession rate as given by eq. (A1-c) would then be

$$\dot{\psi}_r = 1 - \frac{D_f}{2\left(D_f + D_s\right)}.$$

With the aid of the definition (A16-d) and (A16-c) $\dot{\psi}_r = B/D$. Sub- stituting this result in eq. (24-a) (note that γ_r can take any arbitrary value) we get at stability threshold

$$IB^2 - I_z BD = KD^2 \tag{26}$$

which is precisely identical to the result obtained earlier in eq. (22) using the classical Routh-Hurwitz criterion.

Suppose that the relationship between the transverse and the polar moments of inertia, I and I_z, respectively, is given by

$$I = cI_z$$

where $c = 1/2$ is the geometrical lower bound for cylindrical rigid bodies. Reorganizing condition (21) using the above geometrical relationship results in

$$I\left(B - \frac{D}{c}\right) < \frac{KD^2}{B} \tag{27}$$

where the right hand side is positive by virtue of fulfilling the previous conditions on the overall stiffness K. Obviously when the left hand side is non-positive, dynamic stability is geometrically guaranteed by

$$c \le \frac{D}{B} = \frac{D_s + D_f}{D_s + \frac{1}{2} D_f} \tag{28}$$

providing an upper bound for c, and as can be seen, it is solely composed by the two damping coefficients in the system. When the support damping, D_s, is absent, the requirement on c is

$$\frac{1}{2} \le c \le 2 \tag{29-a}$$

In the other extreme, when $D_s >> D_f$, then

$$\frac{1}{2} \le c \le 1 \tag{29-b}$$

We see immediately that high support damping relative to fluid damping is undesirable since it reduces the range of c which guarantees stability. Still, in either case the two lower limits indicate that a thin flexibly-mounted rotor ("short disk"), or c = 1/2, guarantees dynamic stability. This is due to the gyroscopic effect that tends to decrease rotor nutation. If, on the other hand, c violates condition (28), or if the flexibly-mounted rotor is very long compared to its diameter (c is large), then the gyroscopic couple tends to completely rotate the rotor about its diameter an angle of $\pi/2$. Hence, the system may be unstable about $\gamma_r = 0$. To also guarantee stability for large c ratios the full condition (21) must be considered. Using dimensional variables (see nomenclature) in equation (22) results in the critical speed

$$\omega_{cr}^{2} = \frac{K^* D^{*2}}{I^* B^{*2} - I_z^* B^* D^*} \tag{30}$$

where according to condition (21), stable operation is guaranteed at any $\omega < \omega_{cr}$. To investigate the role of damping we define a damping ratio $d = D_s/D_f$. Reorganizing eq. (30) using eqs. (A16-d) and (A16-e), we have

$$\frac{\omega_{cr}^{2} I^*}{K^*} = \frac{c\left(d+1\right)^2}{c\left(d+\frac{1}{2}\right)^2 - \left(d+\frac{1}{2}\right)\left(d+1\right)} \tag{31}$$

Fig. 5 shows the behavior of the normalized critical speed in eq. (31) as a function of the geometry ratio, c, with the damping ratio, d, being the parameter. The two extreme cases, d = 0 and d = ∞, are again of special interest. Substituting these cases into eq. (31) results in corresponding critical speeds

$$\omega_0^{2} = \frac{K^*}{I^*}\,\frac{4c}{c-2} = 4\,\frac{K^*}{I^* - 2I_z^*} \tag{32-a}$$

for d = 0, and

$$\omega_\infty^2 = \frac{K^*}{I^*}\ \frac{c}{c-1} = \frac{K^*}{I^* - I_z^*} \qquad (32\text{-b})$$

for d = ∞. The ratio between the two extreme values is

$$\frac{\omega_0^2}{\omega_\infty^2} = 4\ \frac{c-1}{c-2} \qquad (32\text{-c})$$

which results in

$$\frac{\omega_0}{\omega_\infty} > 2 \quad @\ c > 2 \qquad (32\text{-d})$$

This result indicates that whenever $c > 2$, the critical speed for the case $D_s/D_f = 0$ is at least twice as high as the critical speed for the case $D_s/D_f = \infty$. This analysis clearly demonstrates once again that support damping is undesirable since it reduces the value of the critical speed.

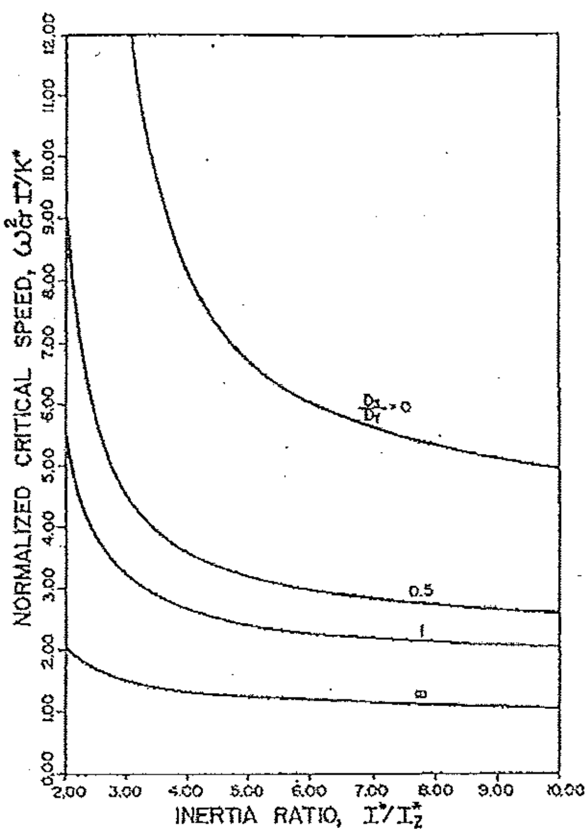

FIG. 5. NORMALIZED CRITICAL SPEED vs. INERTIA RATIO, C, AT VARIOUS DAMPING RATIOS, D_s/D_f

The equations of motion in the axial and angular modes have been constructed for a noncontacting mechanical face seal of the flexibly-mounted rotor type. The equations were expressed in both inertial and rotating references. From these equations we identified the stator and rotor misalignments to be forcing functions. Hence, the stability investigation was performed on the homogeneous part of the equations as if the stator and rotor were perfectly aligned with respect to the axis of shaft rotation.

The stability analysis was performed in the axial and angular modes separately, since the two modes are decoupled when motions are "small." The stability requirement in the axial mode (see eq. (15)) can be summarized as requiring positive axial fluid stiffness; i.e., the pressure drop should induce flow in a converging gap. Hence some coning of the faces is required. The analysis in the angular mode reveals three conditions for stability:

1. The coning angle, according to eq. (19), must be greater than a critical value in order to produce positive angular fluid stiffness in an inward flow regime, and either
2. the rotor should be a "short disk," or
3. the shaft angular speed must be less than a critical value. (At stability threshold the rotor is backward whirling).

If one of the above conditions is violated, then the system will fail in either face contact or excessive leakage due to an exponential growth in the axial displacement and/or rotor nutation.

A comparative study of the two extreme cases, when the support damping is very small compared to fluid film damping, and vice versa, is summarized in Table 2. This table, derived from eqs. (29) and (32), reveals that in the range $1/2 \leq c \leq 1$, which corresponds to a rotor being a "very short disk," stability is guaranteed due to the gyroscopic effect and should be preferred whenever stability is of consideration. In the second range, $1 < c \leq 2$, stability problems may occur when the support damping cannot be neglected. In Fig. 5 the ordinate $c = 2$ is an asymptote to the curve $D_s/D_f = 0$, while at the other extreme ($D_s/D_f = \infty$) and intermediate cases, there already exists a critical speed above which the system will become dynamically unstable. In the range $c > 2$ it is clear from Fig. 5 and Table 2 that support damping has a negative influence on the dynamic stability and can be interpreted as being "internal damping," since it originates from the interface between the rotating shaft and the flexibly-mounted rotor.

Table 2: Critical speed, ω_{cr}, at the two limits of D_s/D_f

c (range)	$D_s/D_f \to 0$	$D_s/D_f \to \infty$
$\frac{1}{2} \leq c \leq 1$	stability guaranteed	stability guaranteed
$1 < c \leq 2$	stability guaranteed	$\omega_\infty^2 = K^*/(I^* - I_x^*)$
$2 < c$	$\omega_0^2 = 4\,K^*/(I^* - 2I_x^*)$	$\omega_\infty^2 = K^*/(I^* - I_x^*)$
	$\omega_0^2/\omega_\infty^2 = 4\,(c-1)/(c-2)$; $\omega_0/\omega_\infty > 2$	

ACKNOWLEDGMENT

This work is based upon the work supported by the National Science Foundation under Grant Number MSM-8619190. This support is gratefully acknowledged.

NOMENCLATURE

B	=	dimensionless damping parameter, eq. (A16-e)
C	=	centerline clearance, $C_o (1 + Z^*)$
C_o	=	design clearance
D^*	=	damping coefficient
D	=	dimensionless damping coefficient; angular $D^*_{11}\omega C_o/Sr_o^4$, axial $D^*_{33}\omega C_o/Sr_o^2$
F^*	=	force
F	=	dimensionless force F^*/Sr_o^2
h	=	local film thickness
I^*	=	rotor momenta of inertia; transverse I^*, polar I^*_z
I	=	dimensionless moment of inertia, $I^*\omega^2C_o/Sr_o^4$
K^*	=	stiffness coefficient
K	=	dimensionless stiffness coefficient; angular $K^*_{11}C_o/Sr_o^4$, axial $K^*_{33}C_o/Sr_o^2$
M^*	=	applied moment
M	=	dimensionless applied moment, M^*/Sr_o^3
m^*	=	rotor mass
m	=	dimensionless mass, $m^*\omega^2C_o/Sr_o^2$
P	=	dimensionless pressure, p/S
p	=	pressure
R	=	dimensionless radial coordinate, r/r_o
r	=	radial coordinate
S	=	seal parameter, $6\mu\omega(r_o/C_o)^2 (1 - R_i)^2$
T^*	=	dynamic moment
T	=	dimensionless dynamic moment, T^*/Sr_o^3
β^*	=	face coning
β	=	dimensionless coning, $\beta^* r_o/C_o$
γ^*	=	misalignment
γ	=	dimensionless misalignment, $\gamma^* r_o/C_o$
μ	=	viscosity
ω	=	shaft angular velocity

Subscripts

cr	=	critical
f	=	fluid film
i	=	inner radius
m	=	mid radius
o	=	outer radius
r	=	rotor
s	=	stator, or flexible support

Arnold, R. N., and Maunder, L., 1961, Gyrodynamics and its Engineering Applications, Academic Press, New York.

Basu, P., and Hughes, W. F., 1987, "Thermal Instability in Two Phase Face Seals," BHRA, Proceedings of the 11th International Conference on Fluid Sealing, pp. 413-441.

Doust, T. G., and Parmer, A., 1987, "Transient Thermoelastic Effects in a Mechanical Face Seal," BHRA, Proceedings of the 11th International Conference on Fluid Sealing, pp. 407-422.

Etsion, I., 1982, "A Review of Mechanical Face Seal Dynamics," The Shock and Vibration Digest, Vol. 14, No. 3, pp. 9-14.

Etsion, I., 1985, "Mechanical Face Seal Dynamics Update," The Shock and Vibration Digest, Vol. 17, No. 4, pp. 11-15.

Green, I., and Etsion, I., 1983, "Fluid Film Dynamic Coefficients in Mechanical Face Seals," Transactions of ASME, Journal of Lubrication Technology, Vol. 105, No. 2, pp. 297-302.

Green, I., and Etsion, I., 1985, "Stability Threshold and Steady-State Response of Noncontacting Coned-Face Seals," ASLE Transactions, Vol. 28, No. 4, pp. 449-460.

Green, I., and Etsion, I., 1986a, "Nonlinear Dynamic Analysis of Noncontacting Coned-Face Mechanical Seals," ASLE Transactions, Vol. 29, No. 3, pp. 383-393.

Green, I., and Etsion, I. 1986b, "Pressure and Squeeze Effects on the Dynamic Characteristics of Elastomer O-Rings Under Small Reciprocating Motion," Transactions of ASME, Journal of Tribology, Vol. 108, No. 3, pp. 439-445.

Green, I., and Etsion, I., 1986c, "A Kinematic Model for Mechanical Seals with Antirotation Locks or Positive Drive Devices," Transactions of ASME, Journal of Tribology, Vol. 108, No. 1, pp. 42-45.

Green, I., 1987, "The Rotor Dynamic Coefficients of Coned-Face Mechanical Seals with Inward or Outward Flow," Transaction of ASME Journal of Tribology, Vol. 109, No. 1, pp. 129-135.

Hughes, W. F., and Chao, N. H., 1980, "Phase Change in Liquid Face Seals II - Isothermal and Adiabatic Bounds with Real Fluids," Transactions of ASME, Journal of Lubrication Technology, Vol. 102, No. 3, pp. 350-359.

Meriam, J. L. 1971, Dynamics, 2nd Edition, John Wiley & Sons, Inc., New York.

Metcalfe, R., 1981, "Dynamic Tracking of Angular Misalignment in Liquid-Lubricated End-Face Seals," ASLE Transactions, Vol. 24, No. 4, pp. 509-516.

Nau, B. S., 1981, "Vibration and Rotary Mechanical Seals," Tribology International, pp. 55-59.

APPENDIX A: THE EQUATIONS OF MOTION IN THE ANGULAR MODE

To obtain the equations of motion in the inertial system $\xi\eta\varsigma$ we have to transform the applied moments given in systems xyz and 123 to system $\xi\eta\varsigma$. Fig. 4 will be used extensively throughout this derivation.

Starting with the flexible support, the applied moments given in eqs. (10-b) and (10-c) have the dimensionless form

$$M_{sx} = - K_s\gamma_r - D_s\gamma_r \qquad \text{(A1-c)}$$

$$M_{sy} = - D_s\dot{\psi}\gamma_r = - D_s \left(\dot{\psi}_r - 1\right) \gamma_r \qquad \text{(A1-b)}$$

where K_{s12} is given in eq. (8-c) and $\dot{\psi}$ is solved from the time derivative of eq. (1):

$$\dot{\psi}_r = 1 + \dot{\psi} \qquad \text{(A1-c)}$$

where the derivatives are taken with respect to the normalized time, ωt. These moments are transformed to the inertial system by

$$M_{s\xi} = M_{sx}\cos\psi_r - M_{sy}\sin\psi_r \qquad \text{(A2-a)}$$

$$M_{s\eta} = M_{sx}\sin\psi_r + M_{sy}\cos\psi_r \qquad \text{(A2-b)}$$

Transforming the rotor nutation, γ_r, to two cartesian tilts yields,

$$\gamma_\xi = \gamma_r\cos\psi_r \qquad \text{(A3-a)}$$

$$\gamma_\eta = \gamma_r\sin\psi_r \qquad \text{(A3-b)}$$

The time derivative of the two tilts is

$$\dot{\gamma}_\xi = \dot{\gamma}_r\cos\psi_r - \dot{\psi}_r\gamma_r\sin\psi_r \qquad \text{(A4-a)}$$

$$\dot{\gamma}_\eta = \dot{\gamma}_r\sin\psi_r + \dot{\psi}_r\gamma_r\cos\psi_r \qquad \text{(A4-b)}$$

Substituting eqs. (A1) in (A2) and using eqs. (A3) and (A4) results finally in

$$M_{s\xi} = - K_s\gamma_\xi - D_s\dot{\gamma}_\xi - D_s\gamma_\eta \qquad \text{(A5-a)}$$

$$M_{s\eta} = - K_s\gamma_\eta - D_s\dot{\gamma}_\eta + D_s\gamma_\xi \qquad \text{(A5-b)}$$

From eqs. (11-b) and (11-c) the fluid film moments are

$$M_{f1} = -K_f\gamma - D_f\dot{\gamma} \tag{A6-a}$$

$$M_{f2} = -K_{f12}\gamma = -D_f\left(\dot{\phi}_1 + \frac{1}{2}\right)\gamma \tag{A6-b}$$

It is more convenient to transform the fluid film moments from system 123 to system xyz and then use the previous steps to further transform them to system $\xi\eta\varsigma$. Hence,

$$M_{fx} = M_{f1}\cos\rho - M_{f2}\sin\rho \tag{A7-a}$$

$$M_{fy} = M_{f1}\sin\rho + M_{f2}\cos\rho \tag{A7-b}$$

where

$$\rho = \phi_1 - \psi \tag{A7-c}$$

$$\rho' = \psi_r - \psi_s \tag{A7-d}$$

The components of the relative misalignment, γ, on axes x and y are

$$\gamma_x = \gamma\cos\rho = \gamma_r - \gamma_s\cos\rho' \tag{A8-a}$$

$$\gamma_y = \gamma\sin\rho = \gamma_s\sin\rho' \tag{A8-b}$$

where the second equality falls out from the definition of eq. (9) and Fig. 4. The time derivative of eqs. (A8) is

$$\dot{\gamma}_x = \dot{\gamma}\cos\rho - \gamma\left(\dot{\phi}_1 - \dot{\psi}\right)\sin\rho \tag{A9-a}$$

$$\dot{\gamma}_y = \dot{\gamma}\sin\rho + \gamma\left(\dot{\phi}_1 - \dot{\psi}\right)\cos\rho \tag{A9-b}$$

which can be reorganized, using eqs. (A8), as

$$\dot{\gamma}\cos\rho - \gamma\dot{\phi}_1\sin\rho = \dot{\gamma}_x - \dot{\psi}\gamma_y \tag{A10-a}$$

$$\dot{\gamma}\sin\rho + \gamma\dot{\phi}_1\cos\rho = \dot{\gamma}_y + \dot{\psi}\gamma_x \tag{A10-b}$$

From eqs. (A8) it is also true that

$$\dot{\gamma}_x = \dot{\gamma}_r + \gamma_s \dot{\psi}_r \sin\rho' \tag{A11-a}$$

$$\dot{\gamma}_y = \gamma_s \dot{\psi}_r \cos\rho' \tag{A11-b}$$

Substituting eqs. (A6) in (A7) and using eqs. (A8) through (A11) along with eq. (A1-c) we get

$$M_{fx} = - K_f \gamma_r - D_f \dot{\gamma}_r + \gamma_s \left(K_f \cos\rho' - \frac{1}{2} D_f \sin\rho' \right) \tag{A12-a}$$

$$M_{fy} = - D_f \left(\dot{\psi}_r - \frac{1}{2} \right) \gamma_r - \gamma_s \left(K_f \sin\rho' + \frac{1}{2} D_f \cos\rho' \right) \tag{A12-b}$$

Now comes the stage of transforming the moments to the inertial system. However, it is useful to note that the terms involving γ_r in eqs. (A12) are similar to those of eqs. (A1). Hence they can be transformed just by replacing subscript s with subscript f in eqs. (A5) and correcting for the coefficient 1/2. The transformation (A2) would then yield

$$M_{f\xi} = - K_f \gamma_\xi - D_f \dot{\gamma}_\xi - \frac{1}{2} D_f \gamma_\eta$$

$$+ \gamma_s \left[\left(K_f \cos\rho' - \frac{1}{2} D_f \sin\rho' \right) \cos\psi_r + \left(K_f \sin\rho' + \frac{1}{2} D_f \cos\rho' \right) \sin\psi_r \right] \tag{A13-a}$$

$$M_{f\eta} = - K_f \gamma_\eta - D_f \dot{\gamma}_\eta + \frac{1}{2} D_f \gamma_\xi$$

$$+ \gamma_s \left[\left(K_f \cos\rho' - \frac{1}{2} D_f \sin\rho' \right) \sin\psi_r - \left(K_f \sin\rho' + \frac{1}{2} D_f \cos\rho' \right) \cos\psi_r \right] \tag{A13-b}$$

With the aid of trigonometric identities and eq. (A7-d), we finally get

$$M_{f\xi} = - K_f \gamma_\xi - D_f \dot{\gamma}_\xi - \frac{1}{2} D_f \gamma_\eta + \gamma_s \left(K_f \cos\psi_s + \frac{1}{2} D_f \sin\psi_s \right) \tag{A14-a}$$

$$M_{f\eta} = - K_f \gamma_\eta - D_f \dot{\gamma}_\eta + \frac{1}{2} D_f \gamma_\xi + \gamma_s \left(K_f \sin\psi_s - \frac{1}{2} D_f \cos\psi_s \right) \tag{A14-b}$$

The components of M_{Xi} (see eq. (7)) in the inertial system are

$$M_{X\xi} = K_s \gamma_{ri} \cos\omega t \tag{A15-a}$$

$$M_{X\eta} = K_s \gamma_{ri} \sin\omega t \tag{A15-b}$$

The angular equations of motion expressed in the inertial system are obtained by equating the dynamic moments of eqs. (6-a) and (6-b) in the ξ and η directions, respectively, to the sum of the corresponding applied moment components given in eqs. (A5), (A14), and (A15). Thus,

$$I\ddot{\gamma}_\xi + I_z \dot{\gamma}_\eta + D\dot{\gamma}_\xi + B\gamma_\eta + K\gamma_\xi = \gamma_s \left[K_f \cos\phi_s + \frac{1}{2} D_f \sin\phi_s\right] + K_s \gamma_{ri} \cos\omega t \tag{A16-a}$$

$$I\ddot{\gamma}_\eta - I_z \dot{\gamma}_\xi + D\dot{\gamma}_\eta - B\gamma_\xi + K\gamma_\eta = \gamma_s \left[K_f \sin\phi_s - \frac{1}{2} D_f \cos\phi_s\right] + K_s \gamma_{ri} \sin\omega t \tag{A16-b}$$

where

$$K = K_s + K_f \tag{A16-c}$$

$$D = D_s + D_f \tag{A16-d}$$

$$B = D_s + \frac{1}{2} D_f \tag{A16-e}$$

The equations of motion in the rotating system xyz are obtained by equating the dynamic moment of eqs. (2) to the sum of the applied moments as given in eqs. (A1), (A12), and the components of M_{Xi} (eq. (7)) on x and y axes. Hence,

$$I\left[\ddot{\gamma}_r - \dot{\phi}_r^{\,2} \gamma_r\right] + I_z \dot{\phi}_r \gamma_r = -K\gamma_r - D\dot{\gamma}_r + K_s \gamma_{ri} \cos\phi$$

$$+ \gamma_s \left[K_f \cos\rho' - \frac{1}{2} D_f \sin\rho'\right] \tag{A17-a}$$

$$I\left[\ddot{\phi}_r \gamma_r + 2\dot{\phi}_r \dot{\gamma}_r\right] - I_z \dot{\gamma}_r = -D\dot{\phi}\gamma_r - \frac{1}{2} D_f \gamma_r - K_s \gamma_{ri} \sin\phi$$

$$- \gamma_s \left[K_f \sin\rho' + \frac{1}{2} D_f \cos\rho'\right] \tag{A17-b}$$